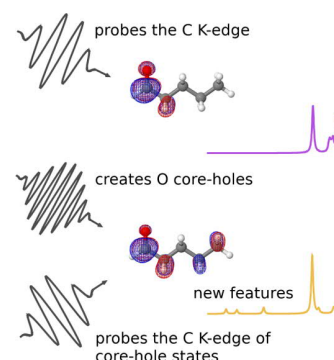


Near-Edge X-ray Absorption Fine Structure Spectroscopy of Heteroatomic Core-Hole States as a Probe for Nearly Indistinguishable Chemical Environments

Daniel R. Nascimento,* Yu Zhang, Uwe Bergmann, and Niranjana Govind*

ABSTRACT: We demonstrate how the near-edge X-ray absorption fine structure (NEXAFS) spectroscopy of single and double core-hole states created by the ionization of a heteroatom can be used to probe subtle changes in intramolecular chemical environments that are nearly indistinguishable by conventional NEXAFS spectroscopy. Using prototypical organic molecules (2/3-pentanone and pentanal), we show how new spectral features emerge in the C K-edge NEXAFS spectra, when creating single and double core-holes at the oxygen heteroatom site. The effect on the lowest unoccupied molecular orbitals is analyzed by studying the double-core-hole-induced ultrafast valence electron dynamics of the three molecules. The predicted changes from our simulations should be observable with state-of-the-art experiments at X-ray free-electron lasers.



When a molecule interacts with an X-ray free electron laser (XFEL) pulse with sufficient peak power and at sufficiently high photon energies, there is a significant probability that one or more of its core electrons will be ionized, leaving behind core-holes. Core-holes can be created either at multiple sites or at a single atomic site, depending on the peak power and frequency range of the XFEL pulse.

A little over three decades ago, Cederbaum et al. demonstrated theoretically that binding energies associated with double core-hole (DCH) states can provide a sensitive platform to probe the varied local atomic environments in molecular systems.^{1,2} These concepts later became the theoretical basis for X-ray two-photon photoelectron spectroscopy (XTPPS),³⁻⁶ predicted to be significantly more sensitive to chemical and many-body effects than conventional X-ray photoelectron spectroscopy (XPS).⁷

The main idea behind XTPPS is that a single X-ray pulse is able to create a DCH via a sequential absorption of two photons, provided that the pulse is intense enough to deliver the necessary number of photons to the volume of interest within the core-hole lifetime. The photoelectrons detected in a suitable energy range will then carry information about the doubly ionized state. Nonetheless, a major difficulty in XTPPS is that its feasibility depends on the availability of intense, ultrafast X-ray pulses. These requirements are difficult to fulfill with synchrotron sources, but routinely achieved at XFEL sources, which have up to 9 orders of magnitude higher peak power.⁸

With the current advances in creating intense, femtosecond X-ray pulses, it has become possible to measure DCH ionization potentials in molecular systems, both at a single site (ss) and at two distinct sites (ts) with the use of X-ray free-electron lasers.⁹⁻¹² ss-DCH and ts-DCH states have also been observed with synchrotron sources,¹³⁻¹⁵ where a single photon ejects an electron with sufficient energy to further ionize the molecule. Note that this process is fundamentally different from the two-photon case discussed in this Letter. The XFEL-based advances have not only demonstrated the feasibility of XTPPS but also opened new avenues to the exploration and development of novel spectroscopies based on core-ionized states both from experimental¹⁶⁻²¹ and theoretical²²⁻²⁸ points of view.

In this Letter, we propose a novel type of spectroscopy based on the near-edge X-ray absorption fine structure (NEXAFS) spectroscopy of molecular systems following core-electron ionization. We envision an experimental setup where two independent ultrafast X-ray laser pulses of different colors are simultaneously applied to a molecular system containing more than one type of atoms. The first pump pulse should be intense enough to create a single core-hole (SCH) or DCH above a specific K-edge (for instance, the oxygen K-edge), while the

second probe pulse should be sufficiently weak to predominantly create SCH states at a different absorption edge (for instance, the carbon edge) that is probed by NEXAFS. Although the first SCH or DCH is localized on a different site than that probed via NEXAFS, its creation can induce an ultrafast charge migration in the valence space,²⁹ leading to significant changes in the final state assessed via NEXAFS. Furthermore, the potential created by the residual positive charge leads to significant changes in the electronic structure of the surrounding atomic sites.

We demonstrate that the creation of SCHs and DCHs at a heteroatomic center in organic molecules can be used as a platform to probe chemical environments that are nearly indistinguishable using traditional NEXAFS spectroscopy.

As a prototypical example, we consider a model system consisting of a set of small ketones/aldehyde isomers of formula $C_5H_{10}O$ as illustrated in Figure 1. This set of

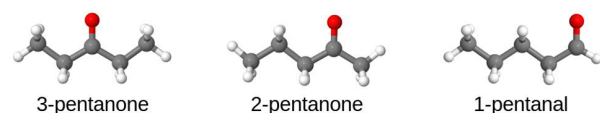


Figure 1. Set of ketones/aldehyde considered in this work. Hydrogen (white), carbon (gray), and oxygen (red).

molecules is interesting as it allows one to explore the emergence and disappearance of spectral features as molecular symmetry is reduced. While 3-pentanone (note that we adopt the IUPAC atom labeling convention for ketones and aldehydes) belongs to the C_{2v} point group, 2-pentanone and pentanal both have C_s symmetry. Thus, changing the position of the oxygen substituent provides a means to explore the gradual effects of symmetry breaking in heterogeneous core-hole spectroscopies.

We begin by analyzing the effect of oxygen core-hole formation (lifetime ≈ 5 fs) (see Computational Details) on the carbon K-edge spectra of the most symmetric molecule, 3-pentanone. In this instance, both methyl and methylene groups are equivalent, and the C K-edge spectra is expected to have only three dominant pre-edge features corresponding to the $C_n 1s \rightarrow \pi^*$ transitions. As shown in Figure 2, the neutral molecule presents the three distinct excitation energies (purple lines), as expected. Nonetheless, these features are separated by only 0.15 eV and thus are very difficult to be distinguished in an experimental setup. Upon the creation of an SCH at the oxygen site, an attosecond valence charge migration is induced, as illustrated in Figure 8. This charge migration plays two important roles in the character of the final core-hole state: (1) it modifies the character of the LUMO as it exchanges hole density with inner valence orbitals, and (2) it leads to a slight destabilization of the carbon core-electrons farther from the oxygen center due to strong attraction with the newly formed core hole. As a consequence, these processes lead to significant changes in the C K-edge spectrum.

In terms of the energy levels, it is possible to observe a much larger separation in the $C_n 1s \rightarrow \pi^*$ transition energies (Figure 2, green lines), with transitions originating from the methyl (C_1) and methylene (C_2) groups being separated by about 1 eV. Because the SCH state is a doublet, it is also possible to observe spin splittings at each pre-edge feature; nonetheless, these splittings are appreciable only at the carbonyl edge (C_3).

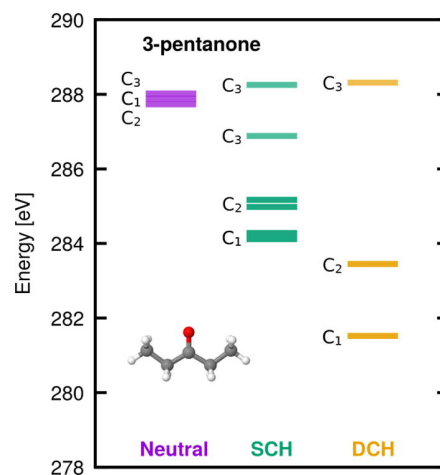


Figure 2. Computed excitation energies for the $C_n 1s \rightarrow \pi^*$ transitions in neutral 3-pentanone and after the creation of SCHs and DCHs at the oxygen site, respectively. Excitation energies were uniformly shifted by +11.4 eV.

With the creation of a ss-DCH, Coulombic interactions are further increased, leading to an even larger separation between the different edges (Figure 2, orange lines). In this case, the distinct pre-edge features appear separated by at least 2 eV, making it possible to distinguish them in an experimental setup. Whether these states are bright or not to be detectable through spectroscopy will depend on the extent to which the LUMO (π^* -orbital) is modified by the DCH formation; for instance, a bright signal is to be expected if there is a large spatial overlap between the resulting LUMO and the core $1s$ orbital localized at a given carbon center.

In Figure 3, we provide the computed C K-edge spectra of 3-pentanone in its neutral state, and after the creation of SCH

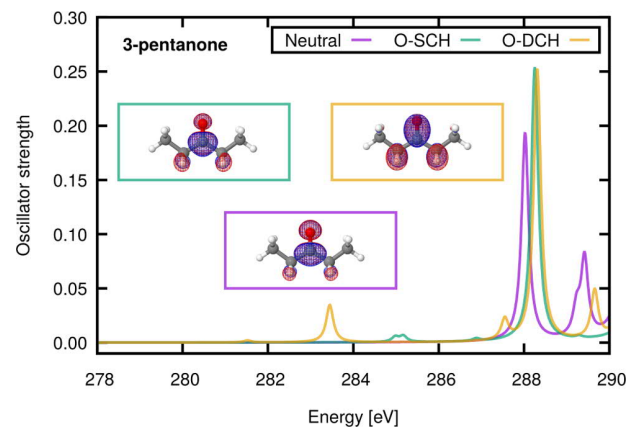


Figure 3. Computed C K-edge spectra for neutral 3-pentanone and after the creation of SCHs and DCHs at the oxygen site, respectively. The inset shows the shape of the LUMO (π^*) in each case. Spectra were uniformly shifted by +11.4 eV.

and DCHs. For the neutral molecule, the LUMO is localized on the carbonyl and methylene groups, and thus, the main pre-edge feature at 288.0 eV is mostly dominated by the $C_3 1s \rightarrow \pi^*$ transition, with a small contribution from the $C_{2,4} 1s \rightarrow \pi^*$. Note that the features above 289 eV correspond to transitions into Rydberg-like states and will not be further discussed in this work. Upon the SCH creation, the LUMO is still localized

at the carbonyl and methylene groups, but with a slightly larger amplitude in the methylene region. This change is evidenced by the appearance of the doublet at 284.9 and 285.2 eV corresponding to the $C_{2,4} 1s \rightarrow \pi^*$ transition. On the other hand, the creation of a DCH leads to dramatic changes in the shape of the LUMO, with large amplitudes around the carbonyl and methylene groups and a smaller amplitude around the methyl groups. Accordingly, the peak corresponding to the $C_{2,4} 1s \rightarrow \pi^*$ transition, now appearing at 283.4 eV becomes a prominent feature in the spectrum, and a small peak at 281.5 eV corresponding to the $C_{1,5} 1s \rightarrow \pi^*$ transition becomes visible.

The picture is very similar in the case of 2-pentanone, with the exception that now the C_{2v} symmetry is broken, and all carbon atoms are nonequivalent. Thus, five distinct signatures are to be expected. Because C_1 and C_3 are almost equidistant from the carbonyl group (C_2), the extent in which these centers are affected by the core-hole creation is similar enough such that no significant separation between the $C_1 1s \rightarrow \pi^*$ and $C_3 1s \rightarrow \pi^*$ transitions is observed. Nonetheless, the identification of five distinct excitation energies can still be made, especially in the DCH state, as shown in Figure 4.

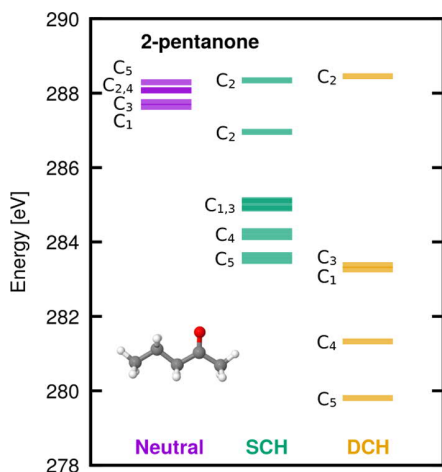


Figure 4. Computed excitation energies for the $C_n 1s \rightarrow \pi^*$ transitions in neutral 2-pentanone and after the creation of SCHs and DCHs at the oxygen site, SCH and DCH, respectively. Excitation energies were uniformly shifted by +11.4 eV.

The C K-edge spectra for 2-pentanone are provided in Figure 5, where one can observe similar features to those presented for 3-pentanone, with the clear exception that the feature around 283.3 eV for the DCH state is now a convolution of two closely spaced peaks at 283.26 and 283.38 eV assigned to the $C_1 1s \rightarrow \pi^*$ and $C_3 1s \rightarrow \pi^*$ transitions, respectively. Note also that the $C_4 1s \rightarrow \pi^*$ transition is virtually invisible as a consequence of the shape of the LUMO.

We now turn our attention to the least symmetric molecule, pentanal. In this case, we expect to see five distinct excitation energies. Although these transitions for the neutral molecule appear all within a 0.7 eV window, the creation of a single O core-hole is sufficient to spread them over a much larger, 6 eV, window, where transition energies are separated by at least 0.4 eV, as illustrated in Figure 6.

As discussed above, the creation of a second core-hole in the oxygen site further increases this separation to at least 0.8 eV.

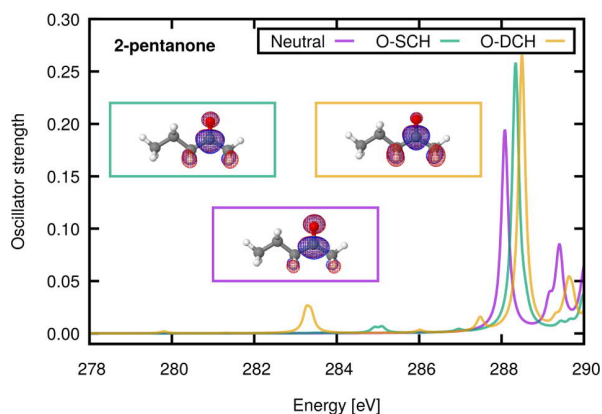


Figure 5. Computed C K-edge spectra for neutral 2-pentanone and after the creation of an SCH and DCH at the oxygen site, respectively. The inset shows the shape of the LUMO (π^*) in each case. Spectra were uniformly shifted by +11.4 eV.

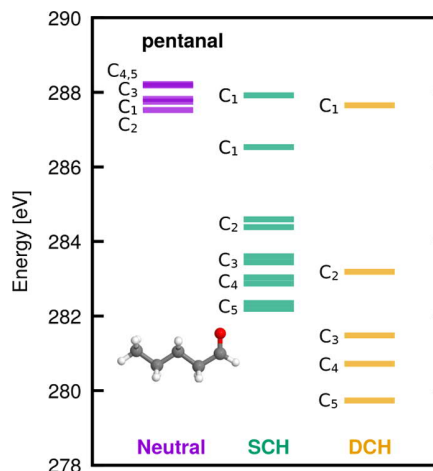


Figure 6. Computed excitation energies for the $C_n 1s \rightarrow \pi^*$ transitions in neutral pentanal and after the creation of an SCH and DCH at the oxygen site, respectively. Excitation energies were uniformly shifted by +11.4 eV.

The most striking difference between the behaviors of pentanal and 2/3-pentanone is in the way in which the LUMOs are modified by the core-hole creation.

As observed in Figure 7, the LUMO for the neutral molecule is localized in the carbonyl center with a small amplitude around C_2 , and thus, the pre-edge feature around 287.7 eV can be assigned to the $C_1 1s \rightarrow \pi^*$ transition with a minor contribution from the $C_2 1s \rightarrow \pi^*$ transition. Similarly, the creation of a SCH induces a larger LUMO amplitude around C_2 , making the $C_2 1s \rightarrow \pi^*$ transition, now at 284.4 and 284.6 eV, slightly more prominent. In this case, DCH creation delocalizes the LUMO throughout the entire molecular backbone, although no amplitude is observed around C_3 . As a consequence, all new pre-edges, with the exception of the $C_3 1s \rightarrow \pi^*$ transition, present rather strong signatures.

Thus, heteroatom DCH K-edge spectroscopy can be a powerful approach in differentiating structural isomers and intramolecular chemical environments that cannot be distinguished by traditional K-edge spectroscopies alone, like for instance, the three methylene groups in pentanal.

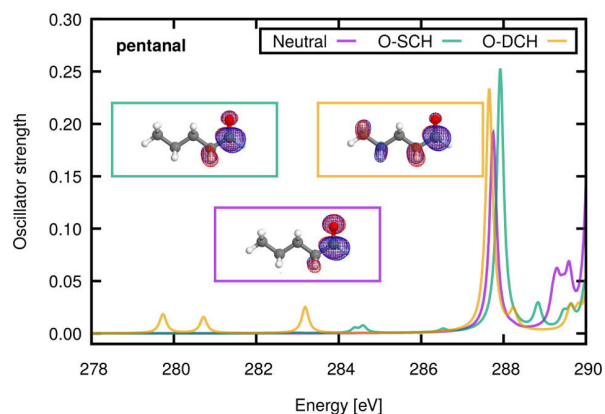


Figure 7. Computed C K-edge spectra for neutral pentanal and after the creation of an SCH and DCH at the oxygen site, respectively. The inset shows the shape of the LUMO (π^*) in each case. Spectra were uniformly shifted by +11.4 eV.

In order to gain a further understanding on how the DCH creation affects the shape of the LUMOs, we performed DCH-induced valence electron dynamics simulations for all three molecules. The results are provided in Figure 8.

As can be seen in Figure 8, the creation of a DCH at the oxygen site induces an attosecond valence dynamics, which in all cases involves the exchange of hole density between the HOMO + sub-HOMO and the LUMO. Note, however, that the HOMOs are orthogonal to all the other orbitals taking place in the dynamics, and their contribution to the hole migration is rather small.

In the case of 3-pentanone, significant hole-density exchange happens only between the HOMO-1 and LUMO, both of π^* symmetry. The linear combination of these two orbitals then leads to the relaxed DCH-LUMO observed in Figure 3 with an enhanced amplitude in the methylene positions and a small amplitude in the methyl groups. A similar conclusion can be drawn in the case of 2-pentanone. For pentanal, however, hole density is exchanged between the HOMO-6 and LUMO and HOMO-4 and LUMO. The relaxed DCH-LUMO is thus expected to have strong contributions from all of these orbitals. If we consider that the HOMO-6 and HOMO-4 are out-of-phase in C_3 and C_5 , and considering that the HOMO-4 interacts more strongly with the LUMO than the HOMO-6 does, it is not difficult to imagine a scenario where the amplitude in C_3 completely vanishes resulting in the relaxed DCH-LUMO observed in Figure 7.

In summary, we have demonstrated that the creation of SCHs and DCHs at a heteroatomic center in an organic molecule can be used as a platform to probe nearly indistinguishable chemical environments, such as several symmetrically nonequivalent carbon centers in organic molecules. We demonstrate that in the case of 2/3-pentanone and pentanal, the emergence of new spectral features in the C K-edge NEXAFS spectra induced by the creation of SCHs and DCHs at the oxygen site can be rationalized in terms of the interaction between the Coulomb hole at the oxygen center and the inner-shell electrons at the carbon centers, leading to a destabilization of carbon core electrons farther from the core-hole site, and the induced valence charge migration that leads to LUMOs with modified shapes.

We appreciate that including nuclear dynamics in our RT-TDDFT simulations may be important as the C-H bond

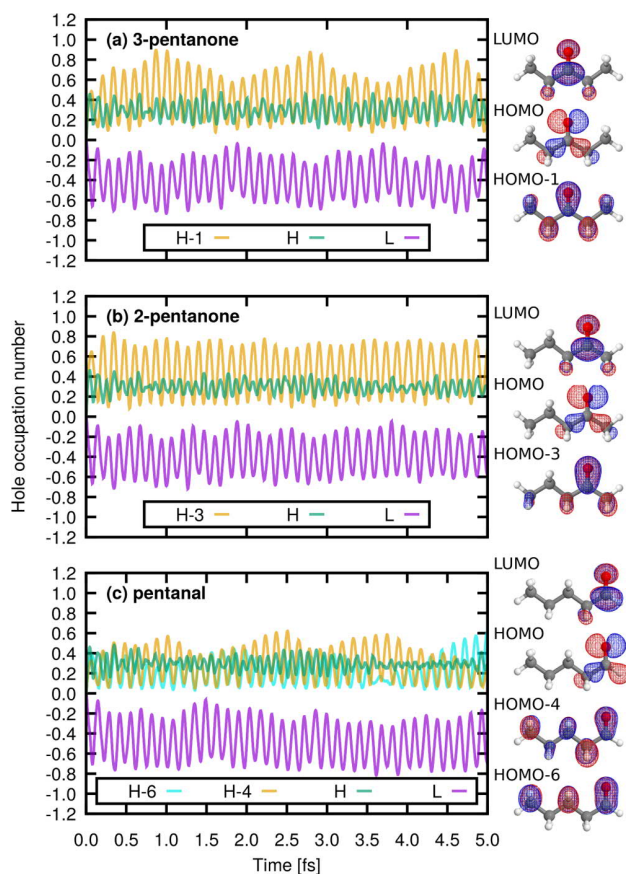


Figure 8. Simulated valence charge migration of 3/2-pentanone and pentanal induced by the creation of a DCH at the oxygen site as measured by the change in the hole occupation number in the relevant MOs. A positive (negative) hole occupation number represents loss (gain) of electronic charge density. The shape of the MOs relevant to the valence electron dynamics are represented in the right panel. Only MOs that contribute with more than $0.2e$ throughout the simulation are shown (H, HOMO; L, LUMO).

stretch is on the order of ~ 11 fs, which is roughly twice the oxygen core-hole lifetime (~ 5 fs). These effects are currently not available in our RT-TDDFT implementation. That being said, the present work is meant to be a proof-of-principle study to highlight the role of single and double core-holes as a means to probe nearly indistinguishable intramolecular chemical environments via NEXAFS. A follow-up study including nuclear motions would be essential to further elucidate our findings.

We note that when performing the two-color experiments to measure the carbon NEXAFS while simultaneously creating an oxygen core-hole, one has to consider the possibility that the second color that creates the oxygen core-hole also creates additional carbon core-holes. This potential artifact can be addressed by tuning the second color to both above and below the threshold for creating an oxygen core-hole. As the cross section for creating a carbon core-hole does not change significantly between, e.g., 535 and 545 eV, any observed difference must come from the absence or presence of the oxygen core-hole. It is also conceivable that by varying the delay between the pump and probe, one can study the influence of the core-hole on the NEXAFS.

The continuous development of new XFELs such as LCLS-II will provide intense, tunable, two-color X-ray pulses^{30,31} at high repetition rates. Thus, we envisage that the work suggested here will become experimentally feasible with the high data quality required to not just observe but quantitate the spectral changes from nonlinear effects. These advances will add a powerful dimension to NEXAFS spectroscopy for characterizing the electronic structure and its dynamics in many molecular systems.

COMPUTATIONAL DETAILS

All C K-edge spectra were computed within the time-dependent density functional theory (TDDFT) framework, employing the 6-311G* basis set,^{32,33} the Tamm–Dancoff approximation,³⁴ the Perdew–Burke–Ernzerhof exchange–correlation functional with 25% of Hartree–Fock exchange (PBE0),^{35,36} and the restricted excitation window approach³⁷ as implemented in a development version of the NWChem package.³⁸

Core-hole states were created by first converging the neutral molecule to its electronic ground state followed by the removal of one or two electrons from the 1s molecular orbital localized in the oxygen atom. These states were subsequently converged to a stationary point by enforcing the population of the O 1s molecular orbital to remain either 1 for SCH or 0 for DCH.

Valence charge migration computations were performed at the real-time TDDFT,³⁹ 6-311G* level of theory, and PBE0 exchange–correlation functional, respectively. Core-hole states were created as described above, with the exception that here we do not perform the reoptimization step after removal of 1s electrons, simulating a “sudden” X-ray ionization at the oxygen K-edge, as discussed in ref 40. The density matrix of the nonstationary core-ionized state was then propagated field-free in the basis of the neutral molecule for 5 fs with time steps of 1.2 as via

$$\frac{\partial}{\partial t} \mathbf{P}'(t) = -i[\mathbf{F}'(t), \mathbf{P}'(t)] \quad (1)$$


where \mathbf{F}' and \mathbf{P}' represent the Fock and density matrices in the MO basis, respectively. Nuclei are kept frozen, and no dissipation is included in the propagation.


The hole-occupation number was then evaluated as

$$n_k(t) = [\mathbf{C}^\dagger \mathbf{P}'(t) \mathbf{C}]_{kk} \quad (2)$$

AUTHOR INFORMATION


Corresponding Authors

Daniel R. Nascimento – Pacific Northwest National Laboratory, Richland, Washington;  orcid.org/0000-0002-2126-8378; Email: daniel.nascimentodasilva@pnnl.gov

Niranjan Govind – Pacific Northwest National Laboratory, Richland, Washington;  orcid.org/0000-0003-3625-366X; Email: niri.govind@pnnl.gov

Other Authors

Yu Zhang – SLAC National Accelerator Laboratory, Menlo Park, California

Uwe Bergmann – SLAC National Accelerator Laboratory, Menlo Park, California;  orcid.org/0000-0001-5639-166X

Notes

The authors declare no competing financial interest.

ACKNOWLEDGMENTS

This material is based on the work supported by the U.S. Department of Energy, Office of Science, Office of Basic Energy Sciences under the Contract Nos. KC030103172684 (D.R.N. and N.G.) and DE-AC02-76SF00515 (Y.Z. and U.B.) including Laboratory Directed Research and Development funding (Y.Z. and U.B.) at SLAC National Accelerator Laboratory. The computational work was performed using EMSL, a DOE Office of Science User Facility sponsored by the Office of Biological and Environmental Research and located at the Pacific Northwest National Laboratory (PNNL). PNNL is operated by Battelle Memorial Institute for the United States Department of Energy under DOE contract number DE-AC05-76RL1830.

REFERENCES

- (1) Cederbaum, L.; Tarantelli, F.; Sgamellotti, A.; Schirmer, J. On double vacancies in the core. *J. Chem. Phys.* **1986**, *85*, 6513–6523.
- (2) Cederbaum, L.; Tarantelli, F.; Sgamellotti, A.; Schirmer, J. Double vacancies in the core of benzene. *J. Chem. Phys.* **1987**, *86*, 2168–2175.
- (3) Santra, R.; Kryzhevoi, N. V.; Cederbaum, L. S. X-ray two-photon photoelectron spectroscopy: a theoretical study of inner-shell spectra of the organic para-aminophenol molecule. *Phys. Rev. Lett.* **2009**, *103*, 013002.
- (4) Tashiro, M.; Ehara, M.; Fukuzawa, H.; Ueda, K.; Buth, C.; Kryzhevoi, N. V.; Cederbaum, L. S. Molecular double core hole electron spectroscopy for chemical analysis. *J. Chem. Phys.* **2010**, *132*, 184302.
- (5) Tashiro, M.; Ehara, M.; Ueda, K. Double core–hole electron spectroscopy for open-shell molecules: Theoretical perspective. *Chem. Phys. Lett.* **2010**, *496*, 217–222.
- (6) Takahashi, O.; Tashiro, M.; Ehara, M.; Yamasaki, K.; Ueda, K. Theoretical Molecular Double-Core-Hole Spectroscopy of Nucleobases. *J. Phys. Chem. A* **2011**, *115*, 12070–12082.
- (7) Siegbahn, K. *Electron Spectroscopy for Chemical Analysis*. Atomic Physics 3: Boston, MA, 1973; pp 493–522.
- (8) Bergmann, U.; Yachandra, V. K.; Yano, J. *X-Ray Free Electron Lasers: Applications in Materials, Chemistry and Biology*; Royal Society of Chemistry, 2017; Vol. 18.
- (9) Fang, L.; Hoener, M.; Gessner, O.; Tarantelli, F.; Pratt, S. T.; Kornilov, O.; Buth, C.; Gühr, M.; Kanter, E. P.; Bostedt, C.; et al. Double Core-Hole Production in N₂: Beating the Auger Clock. *Phys. Rev. Lett.* **2010**, *105*, 083005.
- (10) Berrah, N.; Fang, L.; Murphy, B.; Osipov, T.; Ueda, K.; Kukkk, E.; Feifel, R.; van der Meulen, P.; Salen, P.; Schmidt, H. T.; et al. Double-core-hole spectroscopy for chemical analysis with an intense X-ray femtosecond laser. *Proc. Natl. Acad. Sci. U. S. A.* **2011**, *108*, 16912–16915.
- (11) Salén, P.; van der Meulen, P.; Schmidt, H. T.; Thomas, R. D.; Larsson, M.; Feifel, R.; Piancastelli, M. N.; Fang, L.; Murphy, B.; Osipov, T.; et al. Experimental Verification of the Chemical Sensitivity of Two-Site Double Core-Hole States Formed by an X-Ray Free-Electron Laser. *Phys. Rev. Lett.* **2012**, *108*, 153003.
- (12) Larsson, M.; Salén, P.; van der Meulen, P.; Schmidt, H. T.; Thomas, R. D.; Feifel, R.; Piancastelli, M. N.; Fang, L.; Murphy, B. F.; Osipov, T.; et al. Double core-hole formation in small molecules at the LCLS free electron laser. *J. Phys. B: At., Mol. Opt. Phys.* **2013**, *46*, 164030.

- (13) Diamant, R.; Huotari, S.; Hämäläinen, K.; Kao, C.; Deutsch, M. Cu $K^h\alpha_{1,2}$ hypersatellites: Suprathreshold evolution of a hollow-atom x-ray spectrum. *Phys. Rev. A: At., Mol., Opt. Phys.* **2000**, *62*, 052519.
- (14) Lablanquie, P.; Penent, F.; Palaudoux, J.; Andric, L.; Selles, P.; Carniato, S.; Bučar, K.; Žitnik, M.; Huttula, M.; Eland, J. H. D.; et al. Properties of Hollow Molecules Probed by Single-Photon Double Ionization. *Phys. Rev. Lett.* **2011**, *106*, 063003.
- (15) Lablanquie, P.; Grozdanov, T. P.; Žitnik, M.; Carniato, S.; Selles, P.; Andric, L.; Palaudoux, J.; Penent, F.; Iwayama, H.; Shigemasa, E.; et al. Evidence of Single-Photon Two-Site Core Double Ionization of C_2H_2 Molecules. *Phys. Rev. Lett.* **2011**, *107*, 193004.
- (16) Tamasaku, K.; Nagasono, M.; Iwayama, H.; Shigemasa, E.; Inubushi, Y.; Tanaka, T.; Tono, K.; Togashi, T.; Sato, T.; Katayama, T.; et al. Double Core-Hole Creation by Sequential Attosecond Photoionization. *Phys. Rev. Lett.* **2013**, *111*, 043001.
- (17) Nakano, M.; Selles, P.; Lablanquie, P.; Hikosaka, Y.; Penent, F.; Shigemasa, E.; Ito, K.; Carniato, S. Near-Edge X-Ray Absorption Fine Structures Revealed in Core Ionization Photoelectron Spectroscopy. *Phys. Rev. Lett.* **2013**, *111*, 123001.
- (18) Penent, F.; Nakano, M.; Tashiro, M.; Grozdanov, T.; Žitnik, M.; Carniato, S.; Selles, P.; Andric, L.; Lablanquie, P.; Palaudoux, J.; et al. Molecular single photon double K-shell ionization. *J. Electron Spectrosc. Relat. Phenom.* **2014**, *196*, 38–42 Advances in Vacuum Ultraviolet and X-ray Physics, The 38th International Conference on Vacuum Ultraviolet and X-ray Physics (VUVX2013), University of Science and Technology of China.
- (19) Penent, F.; Nakano, M.; Tashiro, M.; Grozdanov, T.; Žitnik, M.; Bučar, K.; Carniato, S.; Selles, P.; Andric, L.; Lablanquie, P.; et al. Double core hole spectroscopy with synchrotron radiation. *J. Electron Spectrosc. Relat. Phenom.* **2015**, *204*, 303–312 Gas phase spectroscopic and dynamical studies at Free-Electron Lasers and other short wavelength sources.
- (20) Püttner, R.; Goldsztejn, G.; Céolin, D.; Rueff, J.-P.; Moreno, T.; Kushawaha, R. K.; Marchenko, T.; Guillemin, R.; Journal, L.; Lindle, D. W.; et al. Direct Observation of Double-Core-Hole Shake-Up States in Photoemission. *Phys. Rev. Lett.* **2015**, *114*, 093001.
- (21) Marchenko, T.; Goldsztejn, G.; Jänkälä, K.; Travnikova, O.; Journal, L.; Guillemin, R.; Sisourat, N.; Céolin, D.; Žitnik, M.; Kavčič, M.; et al. Potential Energy Surface Reconstruction and Lifetime Determination of Molecular Double-Core-Hole States in the Hard X-Ray Regime. *Phys. Rev. Lett.* **2017**, *119*, 133001.
- (22) Ueda, K.; Takahashi, O. Extracting chemical information of free molecules from K-shell double core-hole spectroscopy. *J. Electron Spectrosc. Relat. Phenom.* **2012**, *185*, 301–311 Special Issue in honor of Prof. T. Darrah Thomas: High-Resolution Spectroscopy of Isolated Species.
- (23) Zhang, Y.; Healion, D.; Biggs, J. D.; Mukamel, S. Double-core excitations in formamide can be probed by X-ray double-quantum-coherence spectroscopy. *J. Chem. Phys.* **2013**, *138*, 144301.
- (24) Takahashi, O.; Ueda, K. Molecular double core-hole electron spectroscopy for probing chemical bonds: C60 and chain molecules revisited. *Chem. Phys.* **2014**, *440*, 64–68.
- (25) Hua, W.; Bennett, K.; Zhang, Y.; Luo, Y.; Mukamel, S. Study of double core hole excitations in molecules by X-ray double-quantum-coherence signals: a multi-configuration simulation. *Chem. Sci.* **2016**, *7*, 5922–5933.
- (26) Gao, C.; Zeng, J.; Yuan, J. Single- and double-core-hole ion emission spectroscopy of transient neon plasmas produced by ultraintense x-ray laser pulses. *J. Phys. B: At., Mol. Opt. Phys.* **2016**, *49*, 044001.
- (27) Zhang, Y.; Bergmann, U.; Schoenlein, R.; Khalil, M.; Govind, N. Double core hole valence-to-core x-ray emission spectroscopy: A theoretical exploration using time-dependent density functional theory. *J. Chem. Phys.* **2019**, *151*, 144114.
- (28) Lee, J.; Small, D. W.; Head-Gordon, M. Excited States via Coupled Cluster Theory without Equation-of-Motion Methods: Seeking Higher Roots with Application to Doubly Excited States and Double Core Hole States. arXiv preprint arXiv:1909.10096; 2019.
- (29) Kuleff, A. I.; Kryzhevoi, N. V.; Pernpointner, M.; Cederbaum, L. S. Core ionization initiates subfemtosecond charge migration in the valence shell of molecules. *Phys. Rev. Lett.* **2016**, *117*, 093002.
- (30) Duris, J.; Li, S.; Driver, T.; Champenois, E. G.; MacArthur, J. P.; Lutman, A. A.; Zhang, Z.; Rosenberger, P.; Aldrich, J. W.; Coffee, R. et al. Tunable Isolated Attosecond X-ray Pulses with Gigawatt Peak Power from a Free-Electron Laser. arXiv preprint arXiv:1906.10649; 2019.
- (31) Driver, T.; Li, S.; Champenois, E. G.; Duris, J.; Ratner, D.; Lane, T.; Rosenberger, P.; Al-Haddad, A.; Averbukh, V.; Barnard, T. et al. Attosecond Transient Absorption Spectroscopy: a ghost imaging approach to ultrafast absorption spectroscopy. arXiv preprint arXiv:1909.07441; 2019.
- (32) Clark, T.; Chandrasekhar, J.; Spitznagel, G. W.; Schleyer, P. V. R. Efficient diffuse function-augmented basis sets for anion calculations. III. The 3-21+G basis set for first-row elements, Li-F. *J. Comput. Chem.* **1983**, *4*, 294–301.
- (33) Krishnan, R.; Binkley, J. S.; Seeger, R.; Pople, J. A. Self-consistent molecular orbital methods. XX. A basis set for correlated wave functions. *J. Chem. Phys.* **1980**, *72*, 650–654.
- (34) Hirata, S.; Head-Gordon, M. Time-dependent density functional theory within the Tamm–Dancoff approximation. *Chem. Phys. Lett.* **1999**, *314*, 291–299.
- (35) Perdew, J. P.; Ernzerhof, M.; Burke, K. Rationale for mixing exact exchange with density functional approximations. *J. Chem. Phys.* **1996**, *105*, 9982–9985.
- (36) Adamo, C.; Barone, V. Toward reliable density functional methods without adjustable parameters: The PBE0 model. *J. Chem. Phys.* **1999**, *110*, 6158–6170.
- (37) Lopata, K.; Van Kuiken, B. E.; Khalil, M.; Govind, N. Linear-Response and Real-Time Time-Dependent Density Functional Theory Studies of Core-Level Near-Edge X-Ray Absorption. *J. Chem. Theory Comput.* **2012**, *8*, 3284–3292.
- (38) Valiev, M.; Bylaska, E.; Govind, N.; Kowalski, K.; Straatsma, T.; Dam, H. V.; Wang, D.; Nieplocha, J.; Apra, E.; Windus, T.; et al. NWChem: A comprehensive and scalable open-source solution for large scale molecular simulations. *Comput. Phys. Commun.* **2010**, *181*, 1477–1489.
- (39) Lopata, K.; Govind, N. Modeling fast electron dynamics with real-time time-dependent density functional theory: application to small molecules and chromophores. *J. Chem. Theory Comput.* **2011**, *7*, 1344–1355.
- (40) Bruner, A.; Hernandez, S.; Mauger, F.; Abanador, P. M.; LaMaster, D. J.; Gaarde, M. B.; Schafer, K. J.; Lopata, K. Attosecond Charge Migration with TDDFT: Accurate Dynamics from a Well-Defined Initial State. *J. Phys. Chem. Lett.* **2017**, *8*, 3991–3996.